ORIGINAL RESEARCH ARTICLE

Inhibition of breast cancer growth via miR-7 suppressing ALDH1A3 activity concomitant with decreasing breast cancer stem cell subpopulation

Meng Pan[1,2*] | Miao Li[1*] | Chengzhong You[3*] | Fengshu Zhao[1] | Mei Guo[1] | Hui Xu[1,4] | Luoyang Li[1] | Ling Wang[1] | Jun Dou[1] (ORCID)

[1]Department of Pathogenic Biology and Immunology, School of Medicine, Southeast University, Nanjing, China

[2]Department of Judicial Identification, Jiangsu Province Hospital, The First Affiliated Hospital of Nanjing Medical University, Nanjing, China

[3]Department of General Surgery, Zhongda Hospital, School of Medicine, Southeast University, Nanjing, China

[4]Department of Gynecology & Obstetrics, Zhongda Hospital, School of Medicine, Southeast University, Nanjing, China

Correspondence
Jun Dou, Department of Pathogenic Biology and Immunology, School of Medicine, Southeast University, 87 Ding Jiaqiao Road, Nanjing, 210009 Jiangsu, China.
Email: njdoujun@seu.edu.cn

Abstract

Breast cancer patients with high expression of aldehyde dehydrogenases (ALDHs) cell population have higher tolerability to chemotherapy since the cells posses a characteristic of breast cancer stem cells (BCSCs) that are resistant to conventional chemotherapy. In this study, we found that the ALDH-positive cells were higher in CD44$^+$CD24$^-$ and CD44$^+$CD24$^-$ESA$^+$BCSCs than that in both BT549 and MDA-MB-231 cell lines but microRNA-7 (miR-7) level was lower in CD44$^+$CD24$^-$ and CD44$^+$CD24$^-$ESA$^+$BCSCs than that in MDA-MB-231 cells. Moreover, miR-7 overexpression in MDA-MB-231 cells decreased ALDH1A3 activity by miR-7 directly binding to the 3′-untranslated region of ALDH1A3; while the ALDH1A3 expression was downregulated in MDA-MB-231 cells, the expressions of CD44 and Epithelium Specific Antigen (ESA) were reduced along with decreasing the BCSC subpopulation. Significantly, enforced expression of miR-7 in CD44$^+$CD24$^-$ESA$^+$BCSC markedly inhibited the BCSC-driven xenograft growth in mice by decreasing an expression of ALDH1A3. Collectively, the findings demonstrate the miR-7 inhibits breast cancer growth via suppressing ALDH1A3 activity concomitant with decreasing BCSC subpopulation. This approach may be considered for an investigation on clinical treatment of breast cancers.

KEYWORDS
ALDH1A3, breast cancer, cancer stem cells, miR-7, subpopulation

1 | INTRODUCTION

Breast cancer is the most prevalent cancer and the leading cause of mortality in women worldwide (Guo et al., 2018; Mu et al., 2018). Inspite of the majority of breast cancer patients being clinically node-negative at diagnosis, the developing of metastases and advanced stages in breast cancer patients remains high (Cai et al., 2014; de Boniface et al., 2018). Approximately 25% patients with the disease eventually reveal the recurrence although the efforts of numerous recent studies have been focused on new treatment strategies of combining surgery, radiotherapy, chemotherapy, and biotherapy. One of reasons is that the breast cancer stem cells (BCSCs), which show the characteristics of self-renewal, multidirectional differentiation, and distant metastasis, are responsible for failure treatment of breast cancer (Choi et al., 2018; Ginestier et al.,

*Meng Pan, Miao Li, and Chengzhong You contributed equally to this study.

2007; Zhou et al., 2009). Therefore, targeting eradication of BCSCs or reducing the BCSC subpopulation is a crucial strategy to achieve effective treatment of breast cancer.

A high activity of aldehyde dehydrogenases (ALDHs) defends intracellular homeostasis by catalyzing the conversion of toxic aldehydes into nontoxic carboxylic acids; whereas ALDH-positive breast cancer cells are closely correlated with higher metastasis and recurrence rates and poor clinical outcome in patients. The cells have been shown to be a biological marker of CSCs in many cancers including breast cancer (Charafe-Jauffret et al., 2010; Lugli et al., 2010; Sterzyńska et al., 2018; Zhou et al., 2018). There is growing body of evidence showing the CD44$^+$CD24$^-$CD44$^+$CD24ESA$^+$ (also called CD326 or EpCAM, epithelial cell adhesion molecule), and ALDHs in breast cancer cells are well-accepted molecular markers of BCSCs (Wang et al., 2012, 2018; Zhang et al., 2014). ALDHs activity is widely used in the identification of BCSCs, which is usually measured with the ALDEFLUOR test and flow cytometry (FCM) analysis (Zhou et al., 2018).

Emerging research has indicated that microRNA-7 (miR-7) is a breast cancer suppressor that inhibited the multiple oncogenes such as SET domain bifurcated 1, epidermal growth factor receptor (EGFR), and Kruppel-like factor-4 (KLF-4), etc., in the breast cancer cell lines (Huynh & Jones, 2014; Jeong et al., 2017). Although we have previously found that the overexpression of miR-7 reduced the BCSC subpopulation and partially reversed epithelial–mesenchymal transition (EMT) in human breast cancer MDA-MB-231 cell line (Zhang et al., 2014), however, the molecular mechanisms have remained unclear. Since the BCSC subpopulation generally affects breast cancer's chemoresistance, progression, metastasis, and recurrence (He et al., 2018; Polonio-Alcalá et al., 2018), a better understanding of the mechanisms of decreasing BCSC subpopulation regulated by miR-7 might shed insight into new therapeutic strategy for treatment of breast cancers.

In this study, we extend the previous study and investigate the mechanisms of miR-7 reducing the BCSC subpopulation in vitro and in vivo mouse model. Our data showed that miR-7 directly reduced ALDH1A3 (ALDH1 family member A3) positive cells and decreased the CD44$^+$CD24$^-$ESA$^+$BCSC subpopulation in MDA-MB-231 cells. Furthermore, enforced expression of miR-7 suppressed the ALDH1A3 activity and the BCSCs-driven xenograft growth in nonobese diabetic/severe combined immunodeficient (NOD/SCID) mice. The study provides an evidence that therapeutic application of cancer inhibitor miR-7 may be a novel therapeutic method for treatment of breast cancer.

2 | MATERIALS AND METHODS

2.1 | Ethical statement

This study was performed with approval of the Animal Care and Use Committee of School of Medicine, Southeast University, China. Full details of approval of the study can be found in the approval ID: 20080925.

2.2 | Cell lines

Human breast cancer BT549, MDA-MB-231, and SK-BR-3 cell lines were obtained from the Cellular Institute in Shanghai, China. BT549 and SK-BR-3 cells were maintained in 1640 medium (Gbico). MDA-MB-231 cells were cultured in Dulbecco's Modified Eagle's Medium. All medium consist of 2 mM L-glutamine, 100 U/ml penicillin, 100 μg/ml streptomycin, and 10% fetal bovine serum.

2.3 | Flow cytometry

To detect the purity of BCSCs and ALDH1 activity, the CD44, CD24, ESA antibodies (eBioscience), and the ALDH1 enzyme assay kit (Invitrogen, Carlsbad, CA) were applied on a FCM (BD Biosciences) according to the manufacturer's instructions and as described previously (Dave et al., 2014; Hosea, Hardiany, Ohneda, & Wanandi, 2018).

2.4 | Reverse transcription quantitative real-time polymerase chain reaction

To test the expression of miR-7, CD44, KLF4, ALDH1A3, and ESA, reverse transcription quantitative real-time polymerase chain reaction (RT-qPCR) analyses were used and performed on an ABI step one plus real-time system (Applied Biosystems). Total cellular RNA was isolated from each sample by using a Qiagen RNeasy kit (Qiagen, Valencia, CA). The messenger RNA (mRNA) levels of the genes of interest were expressed as the ratio of each gene of interest to glyceraldehyde 3-phosphate dehydrogenase mRNA per sample. The complementary DNAs (cDNAs) were amplified by RT-qPCR with primers were listed in Table 1. (Cruz-Lozano et al., 2018; Wang et al., 2015).

2.5 | Dual-luciferase reporter assay

We used the miRcode algorithm (release 6.2, http://www.mircode.org/) to search for miR-RNA target of ALDH1A3. The wild/mutated ALDH1A3 were developed by PCR from human genomic DNA. For luciferase reporter assay, PmirGLO dual-luciferase miRNA target expression vector (psiCHECK2-ALDH1A3-3′-untranslated region (3′-UTR; psiCHECK2-ALDH1A3-3′-UTR-Mut) were used in MDA-MB-231 and SK-BR-3 cells (Wang et al., 2014; Zhang et al., 2014). Luciferase reporter assay was performed using the Dual-Luciferase Reporter Assay System (Promega). The luciferase activity was measured 48 hr posttransfection (Chiyomaru et al., 2013).

2.6 | Western blotting

Approximately 1 × 10^6 MDA-MB-231, Lenti-miR-7-MDA-MB-231, Lentivector-MDA-MB-231 cells, or tumor tissue homogenate were collected and lysed in the protein extraction buffer (Novagen, Madison, WI) by following the manufacturer's protocol. 12% sodium dodecyl sulfate-polyacrylamide gel electrophoresis was performed and proteins (10 μg/lane) were transferred onto a polyvinylidene difluoride membrane blocked with 4% dry milk in Tris-buffered saline

TABLE 1 Primer sequences used for RT-qPCR

Gene		Sequence (5′–3′)
GAPDH	F	GAAGGTGAAGGTCGGAGTCA
	R	TTGAGGTCAATGAAGGGGTC
CD44	F	CCCAGATGGAGAAAGCTCTG
	R	ACTTGGCTTTCTGTCCTCCA
ALDH1A3	F	TCTCGACAAAGCCCTGAAGT
	R	GTCCGATGTTTGAGGAAGGA
KLF4	F	TCTCTTCGTGCACCCACTTG
	R	GGCATGAGCTCTTGGTAATGG
ESA	F	GTGCTGGTGTGTGAACACTG
	R	GAAGTGCAGTCCGCAAACTT
MiR-7	F	ACACTCCAGCTGGGTGGAAGACTAGTGATTT
	R	CTCAACTGGTGTCGTGGAGTCGGCAATTCAGTTGAGACAACAAA

Abbreviations: ALDH, aldehyde dehydrogenase; ESA, epithelium specific antigen; GAPDH, glyceraldehyde 3-phosphate dehydrogenase; KLF, Kruppel-like factor; MiR, microRNA; RT-qPCR, reverse transcription quantitative real-time polymerase chain reaction.

with Tween-20 for 1 hr at 22°C, and then incubated respectively with either the rabbit antibody specific to human ESA or ALDH1A3 (Proteintech, Chicago), KLF4 (Santa Cruz Biotechnology, CA), and CD44 (Proteintech), respectively overnight at 4°C. The antibody dilution was 1:1,000. Immunoreactive bands were detected by Odyssey scanning instrument (LI-COR Odyssey Imaging System; Dou et al., 2012; Wang et al., 2015).

2.7 | Short hairpin RNA sequence design and plasmid transfection

Short hairpin RNA (shRNA) sequences of human ALDH1A3 were designed based on the ALDH1A3 DNA sequence (GenBank no. NM_001128128.2) using the siDESIGN design software (Dharmacon, http://www.thermoscientificbio.com/design-center/) and Block-iTTM RNAi Designer (Invitrogen, Grand island, NY) as well as BLAST (http:// www. ncbi. nlm.nih.gov/BLAST). The target sequence site for ALDH1A3 shRNA includes base pairs of 846–787 bp of the ALDH1A3 cDNA sequence. In addition, one scramble sequence was designed as a negative control. ShRNA sequences are as follows: ALDH1A3-siRNA: 5′-GAAGAGGUAUUGAAUGCUAdTdT-3′, 3′-dTdTCUUCUCCAUAACU UACGAU-5′; scramble-siRNA: 5′-GGCUCUAGAAAAGCCUAUGCdTd T-3′, 3′-dTdTCCGAGAUCUUUUCGGAUACG-5′. All the primers were synthesized by Gene and Technology of China in Shanghai. MDA-MB-231 cells were transiently transfected using Lipofectamine 2000 transfection reagent (Invitrogen) according to the manufacturer's recommendations (Chen, Wang, et al., 2013; Nagle et al., 2018).

2.8 | Magnetic activated cell sorting for preparation of BCSCs

CD44, CD24, and ESA antibodies conjugated to magnetic microbeads (Miltenyi Biotec, Bergisch Gladbach, Germany) were used to obtain the BCSCs from the BT549 and MDA-MB-231 cell lines. The sorting method following the manufacturer's instructions and our previous studies. We named CD44⁺CD24⁻ cells or ESA⁺CD44⁺CD24⁻ cells for BCSCs (Dou

et al., 2007; Yang et al., 2014; Zhang et al., 2014). After having identified the ALDH1A3 activity, we used the ESA⁺CD44⁺CD24⁻BCSCs to perform the succedent experiments in vitro and in vivo.

2.9 | Lentivirus encoding miR-7 infection

To obtain the enforced expression of the miR-7 cells, lentivirus encoding miR-7 or blank vector was infected into MDA-MB-231 as previously described (J. S. Chen et al., 2013; Zhang et al., 2014). The clones with the stable miR-7 expression were selected by GFP expression, and then used in infection of ESA⁺CD44⁺CD24⁻BCSCs.

2.10 | Cell cycle

A total of 1×10^6 ESA⁺CD44⁺CD24⁻BCSCs infected with Lenti-miR-7 recombinant, the Lentivector recombinant, and without infection, were respectively fixed overnight with 70% (w/vol) ice-cold ethanol. Cells were then resuspended in 1 ml of phosphate-buffered saline (PBS) containing 40 μg/mL Annexin-V/propidium iodide (PI) and 500 U/ml RNase A. Following incubation for 30 min in the dark at room temperature, cells were analyzed by FCM using the ModFit software system. The PI fluorescence signal peak versus the integral was used to discriminate G2-M cells from G0-G1 doublets. Cell cycle detection kit was procured from KeyGen Biotech of China (Asharani, Low, Kah Mun, Hande, & Valiyaveettil, 2009).

2.11 | Animal experiment

The healthy female-specific pathogen-free NOD/SCID mice (age 6–7 weeks) and weighing 17–18 g were purchased from the Beijing Weitong Lihua Experimental Animal Technology Co., Ltd., China, and raised in individual ventilated cages at 22–25°C in Experimental Animal Center, School of Medicine, Southeast University. Each NOD/SCID mouse received inoculation of 2×10^5 Lenti-miR-7- BCSCs or BCSCs or Lenti-vec-BCSCs at mouse's right inguinal mammary fat pads, 12 mice were divided to three groups of equal size (four per

group). About 32 days after the injection, the developed tumors were tangible. Tumor formations in the groups were monitored every 3 days by 2-dimensional measurements of individual tumors from each mouse. The mice were also monitored for the tumor-free mice, survival mice, and general health indicators, such as feeding, appearance of fur, and so forth. All tumors were harvested 53 days after implantation. The tumor tissues were applied for the western blotting, RT-qPCR, and immunohistochemistry (IHC) assays. All the experiments were repeated twice (Chen, Zhang, et al., 2013).

2.12 | IHC and image analysis

The methodology used to detect the molecules of Ki67, CylinD1, ALDH1A3, CD44, and ESA by IHC assay. Briefly, 5-μm-thin formalin fixed and paraffin-embedded slides were incubated with the rabbit antimouse/human antibodies specific for Ki67, CylinD1, ALDH1A3, CD44, and ESA overnight at 4°C. The negative control was generated by replacing the primary antibody with PBS. The samples were then labeled with horseradish peroxidas-conjugated streptavidin (Invitrogen) and the chromogenic reaction that was developed using Liquid DAB Substrate Pack according to the manufacturer's instructions. The stained cells in the slides from random and nonoverlapping fields were counted under a magnification of ×200. Image Pro Plus Software 6.0 (Media Cybernetics, CA) was used to semi-quantitatively measure the concentration of these molecule IHC. This procedure, was split into six steps: (a) discovering and surveying the section of interest; (b) adjusting the optical densities; (c) obtaining, transforming and preserving images; (d) amending the background and background staining; (e) configuration of the section of interest to determine the optical density; and (f) examining optical densities. (Hu et al., 2011; Luo, Xie, Wu, Wu, & Gong, 2017).

2.13 | Statistical analysis

Values of interest were presented as the mean plus or minus standard deviation. Statistical comparisons were performed using Student's t test method. $p < .05$ was considered statistically significant.

3 | RESULTS

3.1 | Expressions of ALDH and miR-7 in breast cancer cells

To identify ALDH1A3 expression, we first analyzed the ALDH1A3 activity by FCM in BT549 and MDA-MB-231 cell lines. The results showed that there were more counts of ALDH positive cells in CD44$^+$CD24$^-$ and CD44$^+$CD24$^-$ESA$^+$BCSCs than both BT549 and MDA-MB-231 cells (Figure 1a,b) which are significant difference between the CD44$^+$CD24$^-$BCSCs and BT549 cells (Figure 1e; $p < .0019$) or between the CD44$^+$CD24$^-$ESA$^+$BCSC and MDA-MB-231 cells or CD44$^+$CD24$^-$BCSCs ($p < .0007$ or .006; Figure 1f). We found the ALDH positive cells was more obvious in MDA-MB-231 cells (2.64%) and MDA-MB-231 CD44$^+$CD24$^-$BCSCs (19.17%) than

in BT549 cells (1.01%) and BT549 CD44$^+$CD24$^-$BCSCs (2.13%). Although both MDA-MB-231 and BT549 cell lines are the estrogen receptor (ER$^-$), progesterone receptor (PR$^-$), EGFR2 (HER2$^-$), a triple-negative breast cancer cell lines (Zhang et al., 2014), the BT549 cells may be a weaker malignant cancer cells than MDA-MB-231 cells that contain more ALDH-positive cells.

Interestingly, the ALDH1A3 activity was significantly decreased in MDA-MB-231 cells transiently transfected with miR-7 mimic, or siALDH1A3 but not in the miR-7 mimic control, miR-7 inhibitor control, and miR-7 inhibitor (Figure 1c), or ALDH1A3 negative control (siNC) cells (Figure 1d), which were statistically significant as is shown in Figure 1g. In contrast, the miR-7 expression was a lower in CD44$^+$CD24$^-$ and CD44$^+$CD24$^-$ESA$^+$BCSCs than that in MDA-MB-231 cells, which was statistically significant ($p < .0013$ or .0009) as is shown in Figure 1h.

3.2 | miR-7 inhibits the stem-like molecular expression in MDA-MB-231 cells

To confirm the reducing cancer stem-like molecule ALDH1A3 expression mediated directly by miR-7, we next performed luciferase reporter assays. By TargetScan and miRcode algorithm prediction, we found that *ALDH1A3* was one of the candidate genes and has one site in ALDH1A3-encoded mRNA containing a 3′-UTR element for miR-7 (Figure 2a), then we cloned it into a luciferase reporter vector in MDA-MB-231 and SK-BR-3 cells. The results showed that miR-7 reduced the relative luciferase activity of the wild type vector (Figure 2b), in which the putative miR-7 directly bond the 3′-UTR of ALDH1A3 vector but not the negative control or mutation vector, leading to reduction of ALDH1A3 activity. The results of RT-qPCR and western blot further confirmed that the ALDH1A3 expression was significantly reduced in miR-7 mimic transfected MDA-MB-231 and SK-BR-3 cells compared with the controls as shown in Figure 2c,e.

Since miR-7 has multiple regulator functions, we wanted to know whether the miR-7 would affect the cancer stem-like molecular expression in MDA-MB-231 and SK-BR-3 cells. Figure 2g,h show the stem-like molecule expressions of CD44, ALDH1A3, and KLF-4 were markedly decreased in Lenti-miR-7 transductant compared with the control cells detected by RT-qPCR. The results were further confirmed by western blotting (Figure 2i), in which the bands of CD44, KLF4, and ALDH1A3 were weaker in Lenti-miR-7 transductant than those in the controls, and the difference was statistically significant (Figure 2j). Obviously, Lenti-miR-7 transductant increased significantly the relative level of miR-7 in MDA-MB-231 cells compared with the controls detected by RT-qPCR (Figure 2k).

3.3 | Downregulation of ALDH1A3 reduces the CD44 and ESA expressions in breast cancer cells

Owing to ALDH1A3 activity associated with the BCSC quantification, we down regulated the ALDH1A3 expression by transfection of an expression vector-based small hairpin RNA targeting ALDH1A3 (siALDH1A3) in MDA-MB-231 cells and BCSCs to prove the association that the ALDH1A3 expression is positively related to BCSC
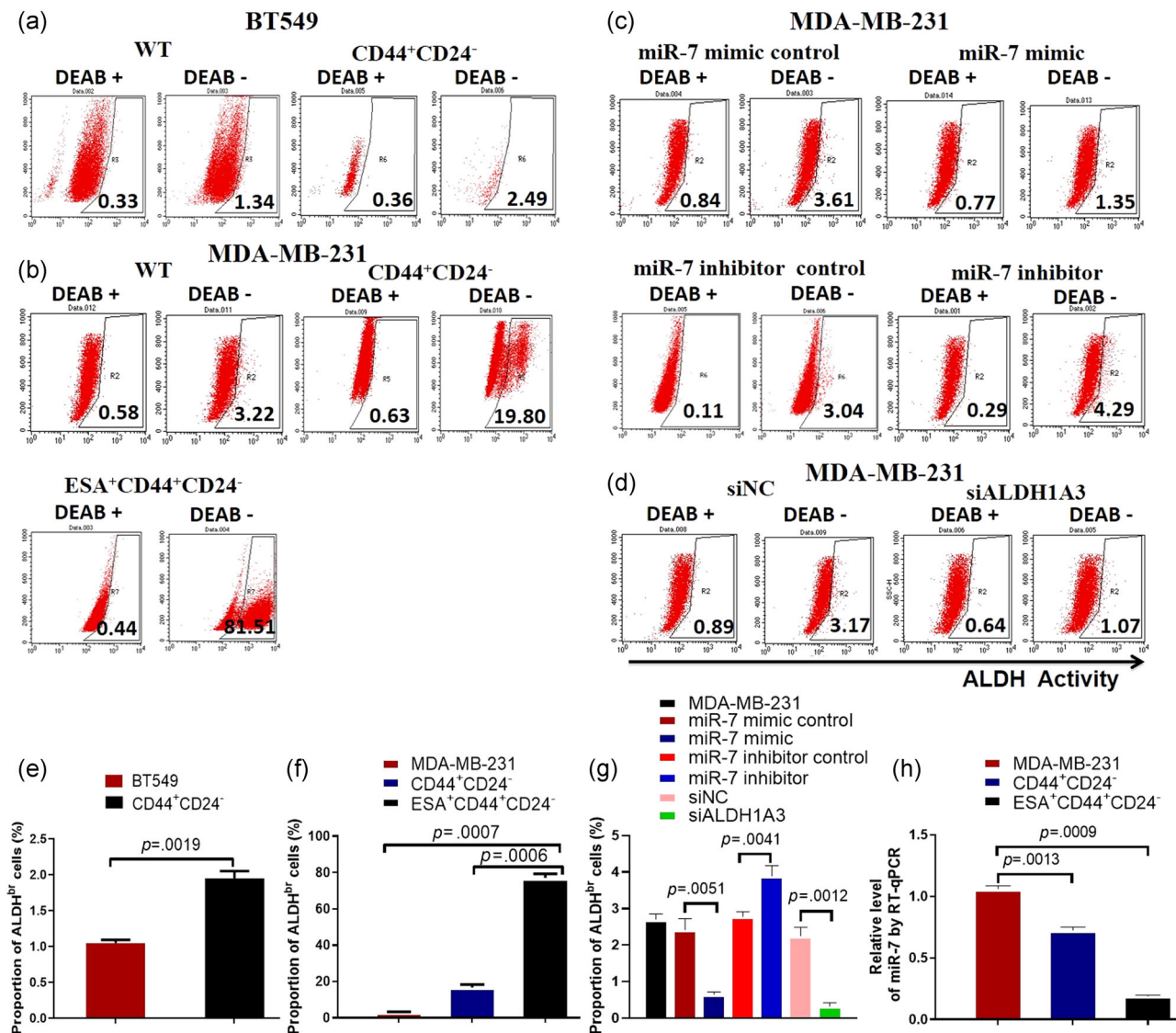
FIGURE 1 Detecting expressions of ALDH and miR-7. FCM analysis of ALDH positive cells. (a) ALDH1 positive cells in BT549 cell line and CD44+CD24−BCSCs isolated from the BT549 cell line. (b) ALDH1A3 positive cells in MDA-MB-231 cell line and CD44+CD24− or CD44+CD24−ESA+BCSCs isolated from the MDA-MB-231 cell line. (c) ALDH positive cells in the MDA-MB-231 cells transiently transfected with miR-7 mimic or different controls. (d) ALDH1 positive cells in MDA-MB-231 cells transiently transfected with siALDH1A3 or ALDH1A3 negative control (siNC). (e) ALDH positive cell proportion in BT549 cells and CD44+CD24−BCSCs analyzed by FCM. (f) ALDH positive cell proportion in MDA-MB-231 cells, CD44+CD24−, and CD44+CD24− ESA+BCSCs analyzed by FCM. (g) ALDH positive cell proportion in MDA-MB-231 cells transfected with miR-7 mimic and different controls or siALDH1A3 and siNC analyzed by FCM. (h) RT-qPCR analysis exhibits the relative level of miR-7 in MDA-MB-231 cells, CD44+CD24−, and CD44+CD24−ESA+BCSCs, respectively. ALDH, aldehyde dehydrogenase; BCSC, breast cancer stem cell; ESA, epithelium specific antigen; FCM, flow cytometry; miR, microRNA; RT-qPCR, reverse transcription quantitative real-time polymerase chain reaction; WT, wild type

subpopulation. FCM analysis indicated that MDA-MB-231 cells transfected with the siALDH1A3 recombinant markedly reduced the expressions of ESA, CD44, and CD44 plus ESA compared with the cells transfected with the siNC or without transfection (Figure 3a,c). The statistical analyses are shown in Figure 3d,f. In addition, the expressions of BCSCs surface markers, the ESA and CD44, were significantly decreased in ESA+CD44+CD24−BCSCs transfected with the siALD-H1A3 recombinant compared with the BCSCs transfected with the siNC (black vector) or without transfection as is shown in Figure 3g, which was statistically significant (Figure 3h). It is thus evident that the

silencing ALDH1A3 in MDA-MB-231 cells and BCSCs definitely reduced the BCSC subpopulation via decrease of CD44 and ESA expressions.

3.4 | Enforced miR-7 expression results in cell cycle arrest

To evaluate the effect of enforced expression of miR-7 on ESA+CD44+CD24−BCSC's growth, we examined the cell cycle process. FCM analysis exhibited that the BCSC-Lenti-miR-7 were
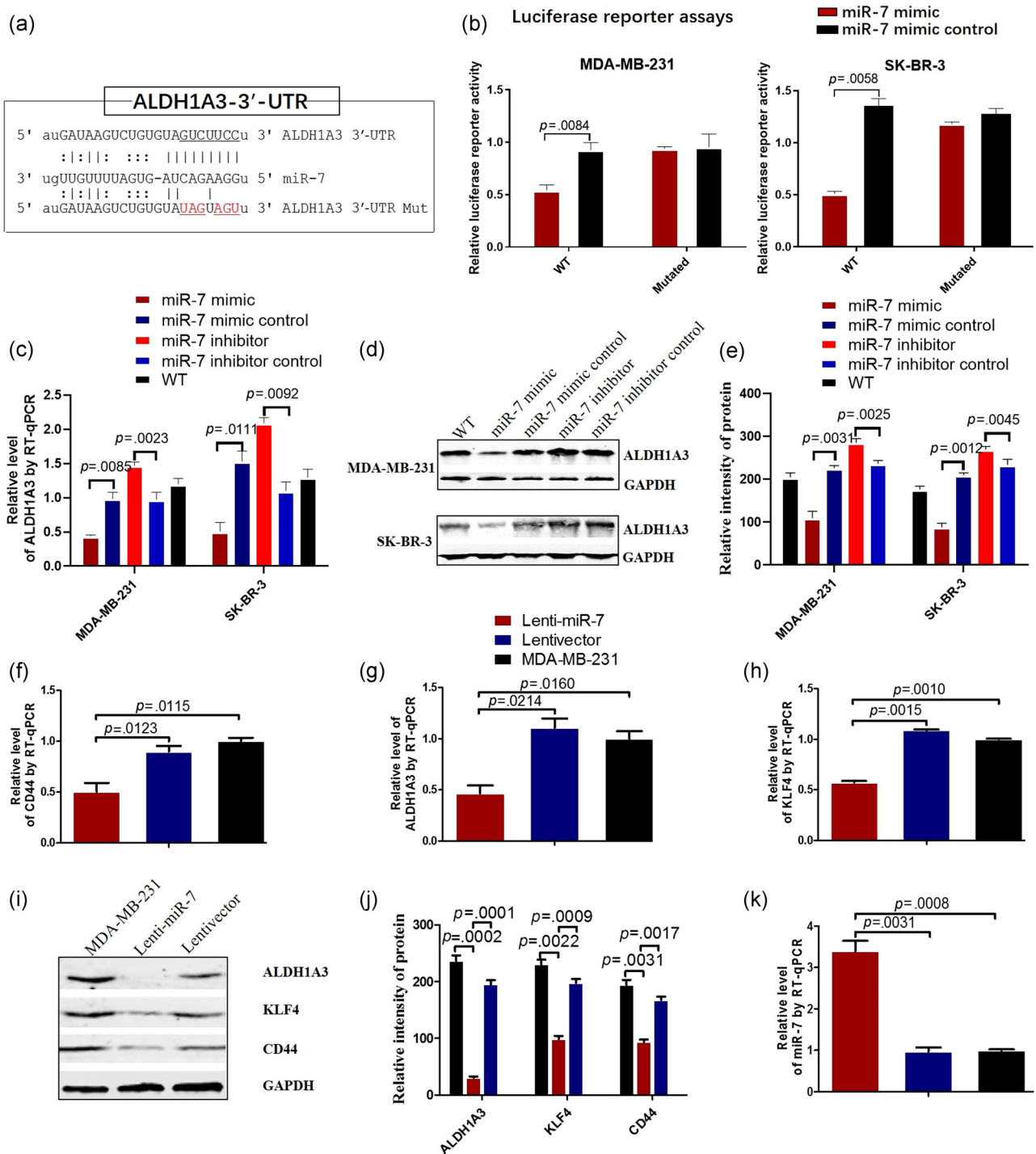
FIGURE 2 MiR-7 reduces the ALDH1A3 activity and the stem-like molecular expression. (a) Putative miR-7 binding and mutated sites in ALDH1A3. (b) Luciferase reporter assay using vectors encoding putative binding sites. MDA-MB-231 and SK-BR-3 cells were transiently transfected with miRNA precursor or negative control, followed by transient transfection with basic vector or wild-type reporter plasmids or mutated plasmids for 48 hr. Reporter activity was measured by luciferase assay. Data are presented as the mean ± *SD*. (c) RT-qPCR analysis indicates the relative level of ALDH1A3 in MDA-MB-231 and SK-BR-3 cells transiently transfected with miR-7 mimic or different controls. (d) ALDH1A3 expression in MDA-MB-231 and SK-BR-3 cells transfected with miR-7 mimic or different controls analyzed by western blot. (e) Semi-quantification analysis of western blot results of ALDH1A3 expression, referring to the differences as indicated. (f–h) RT-qPCR analysis of the stem-like molecular expressions of CD44, ALDH1A3, and KLF4 in MDA-MB-231 cells transfected with miR-7 mimic or controls. (i) The expressions of CD44, ALDH1A3, and KLF4 in MDA-MB-231 cells transfected with miR-7 mimic or controls analyzed by western blot. (j) Semi-quantitative analysis of western blot results, referring to the differences as indicated. (k) RT-qPCR analysis exhibits the miR-7 expression in MDA-MB-231 cells transfected with miR-7 mimic or miR-7 negative control or without transfection. ALDH, aldehyde dehydrogenase; KLF, Kruppel-like factor; miR, microRNA; RT-qPCR, reverse transcription quantitative real-time polymerase chain reaction; *SD*, standard deviation; WT, wild type
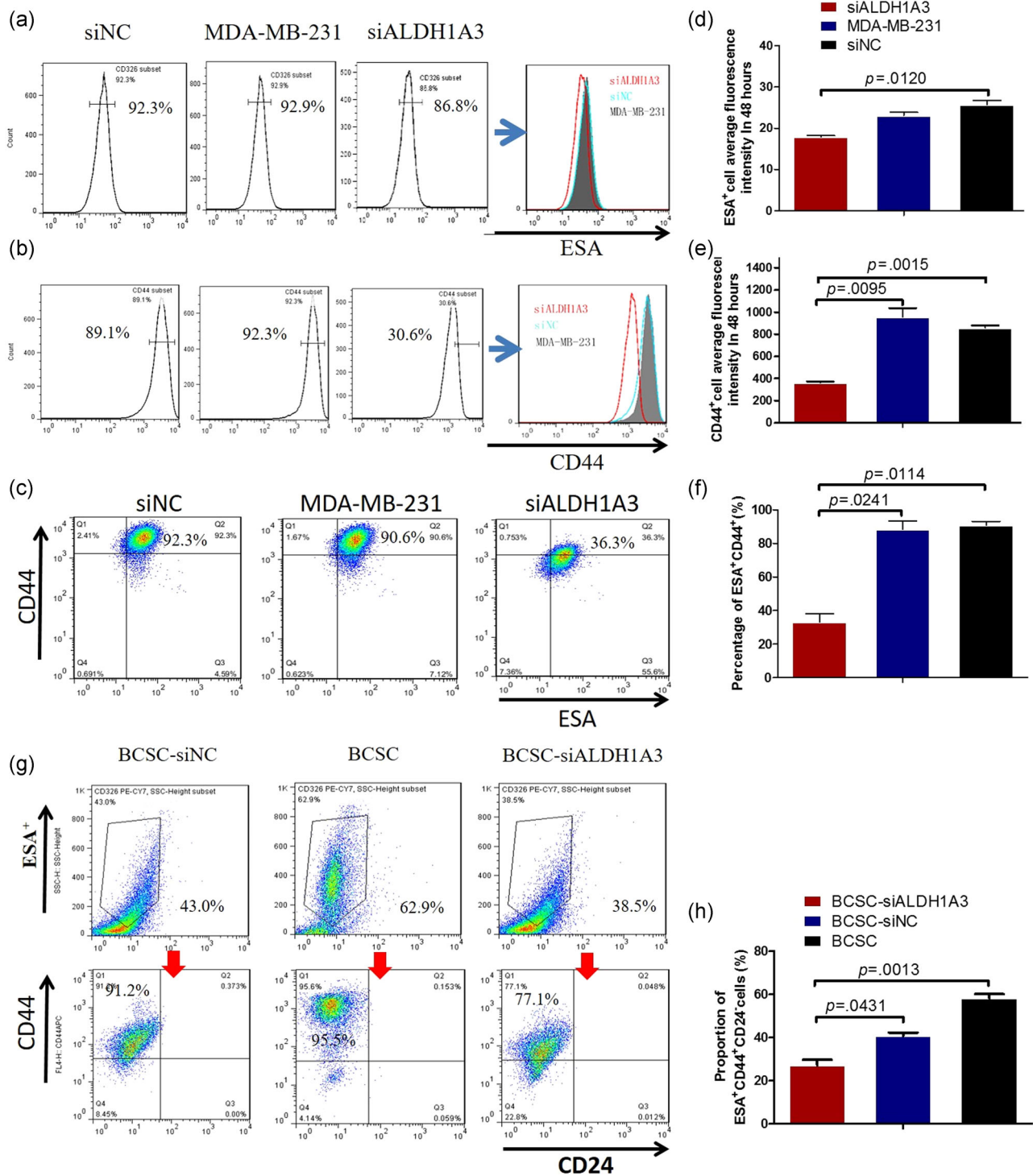
FIGURE 3 Decrease of the CD44$^+$ and ESA$^+$ expressions via downregulated ALDH1A3. (a–c) FCM analysis shows the counts of CD44$^+$, ESA$^+$, and CD44$^+$ plus ESA$^+$ cells in MDA-MB-231 cells transfected with the siALDH1A3 recombinant or the siNC recombinant or without transfection. (d–f) Semi-quantitatively analysis of the FCM results, referring to the differences as indicated. (g) FCM analysis indicates the counts of ESA$^+$CD44$^+$CD24$^-$ cells in BCSCs transfected with the siALDH1A3 recombinant, the siNC recombinant, and without transfection, respectively. (h) Semi-quantitatively analysis of the BCSC counts analyzed by FCM, referring to the differences as indicated. ALDH, aldehyde dehydrogenase; BCSC, breast cancer stem cell; ESA, epithelium specific antigen; FCM, flow cytometry; siNC, ALDH1A3 negative control

significantly increased in the synthesis phase (49.51% vs. 35.77% or 38.02%) and a parallel decreased in the G0-G1 phases (47.48% vs. 55.64% or 53.11%) and the G2-M phases (1.99% vs. 8.12% or 7.60% compared with BCSC-Lentivector and BCSCs, respectively) as shown in Figure 4a–c). Statistical analysis of the different phases was shown in Figure 4d. In addition, we also tested the expressions of Cyclin D1 and Ki67 proteins associated with cell cycles in ESA⁺CD44⁺CD24⁻BCSCs by RT-qPCR (Elliott et al., 2019). The results indicated the expressions of Cyclin D1 and Ki67 were significantly decreased in ESA⁺CD44⁺CD24⁻BCSCs compared with BCSC-Lentivector and BCSCs, respectively (Figure 4e,f), which was further supported by the immunohistochemistry results from the CD44⁺CD24⁻ESA⁺BCSC-driven xenograft tumor tissues as are shown in Figure 4g,h. The results from the experiments well demonstrated that the enforced expression of miR-7 inhibited the proliferation of ESA⁺CD44⁺CD24⁻BCSCs by arresting the cell cycle

process in the G0-G1 and the G2-M phases, suggesting inhibition of ESA⁺CD44⁺CD24⁻BCSC's growth in mice.

3.5 | Enforced miR-7 expression inhibits the BCSCs-derived xenograft growth

After having demonstrated the miR-7 directly inhibited ALDH1A3 expression, decreased the BCSC subpopulation in MDA-MB-231 cells, and induced BCSC's cell cycle arrest in vitro, we wanted to know if miR-7 would inhibit the CD44⁺CD24⁻ESA⁺BCSCs-driven xenograft growth via reducing the ALDH1A3 expression and decreasing the BCSC subpopulation in vivo. Figure 5a gives the sizes of the tumor removed from the tumor bearing mice 53 days after the local injection of 2×10^5 MDA-MB-231CD44⁺CD24⁻ESA⁺BCSCs into NOD/SCID mouse's right inguinal mammary fat pads. All the mice injected with BCSC-Lentivector or BCSCs generated tumors 32 days
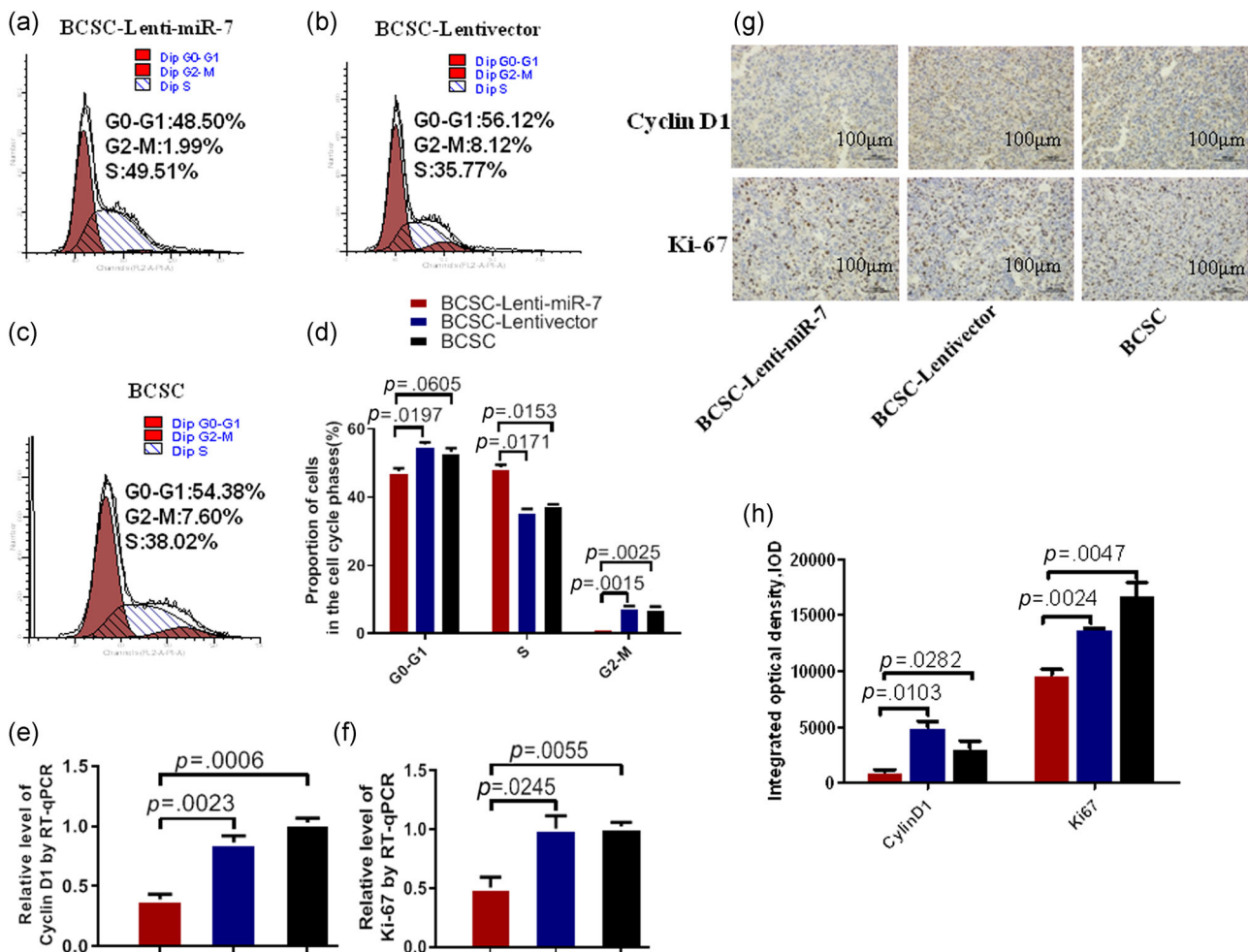

FIGURE 4 MiR-7 inhibits in BCSC's cell cycle. (a–c) FCM analysis show the different phases of cell cycle in ESA⁺CD44⁺CD24⁻BCSCs infected with Lenti-miR-7 recombinant, the Lentivector recombinant, and without infection, respectively. (d) Quantification of the BCSC proportion in the different phases of cell cycle, referring to the differences as indicated. (e and f) RT-qPCR analysis of the expressions of Cyclin D1 and Ki67 in ESA⁺CD44⁺ CD24⁻BCSCs transfected with miR-7 mimic or miR-7 negative control or without transfection. (g) The expressions of Cyclin D1 and Ki67 in ESA⁺ CD44⁺CD24⁻BCSC-driven xenograft tumor tissues, analyzed by IHC. (h) Semi-quantitatively analysis of the Cyclin D1 and Ki67 expressions, referring to the differences as indicated. BCSC, breast cancer stem cell; ESA, epithelium specific antigen; FCM, flow cytometry; IHC, immunohistochemistry; miR, microRNA; RT-qPCR, reverse transcription quantitative real-time polymerase chain reaction

after injection (Figure 5b), the one out of 4 mice injected with Lenti-miR-7 BCSCs developed the visible tumors, however, the measurable tumor was not detected in remaining three mice in the 53-day observation period. (Figures 5a,b). There were a statistically significant differences in tumor sizes between the BCSC-Lenti-miR-7 and BCSC-Lentivector groups, and between the

BCSC-Lenti-miR-7 and BCSC groups (Figure 5b). Figure 5c exhibits the expressions of ALDH1A3, CD44, and ESA in the tumor tissues detected by IHC. We found that the tumor cells from the tumor bearing mice challenged with the BCSC-Lenti-miR-7 markedly decreased the staining of ALDH1A3, CD44, and ESA compared with the tumor cells from the tumor-bearing mice challenged with the
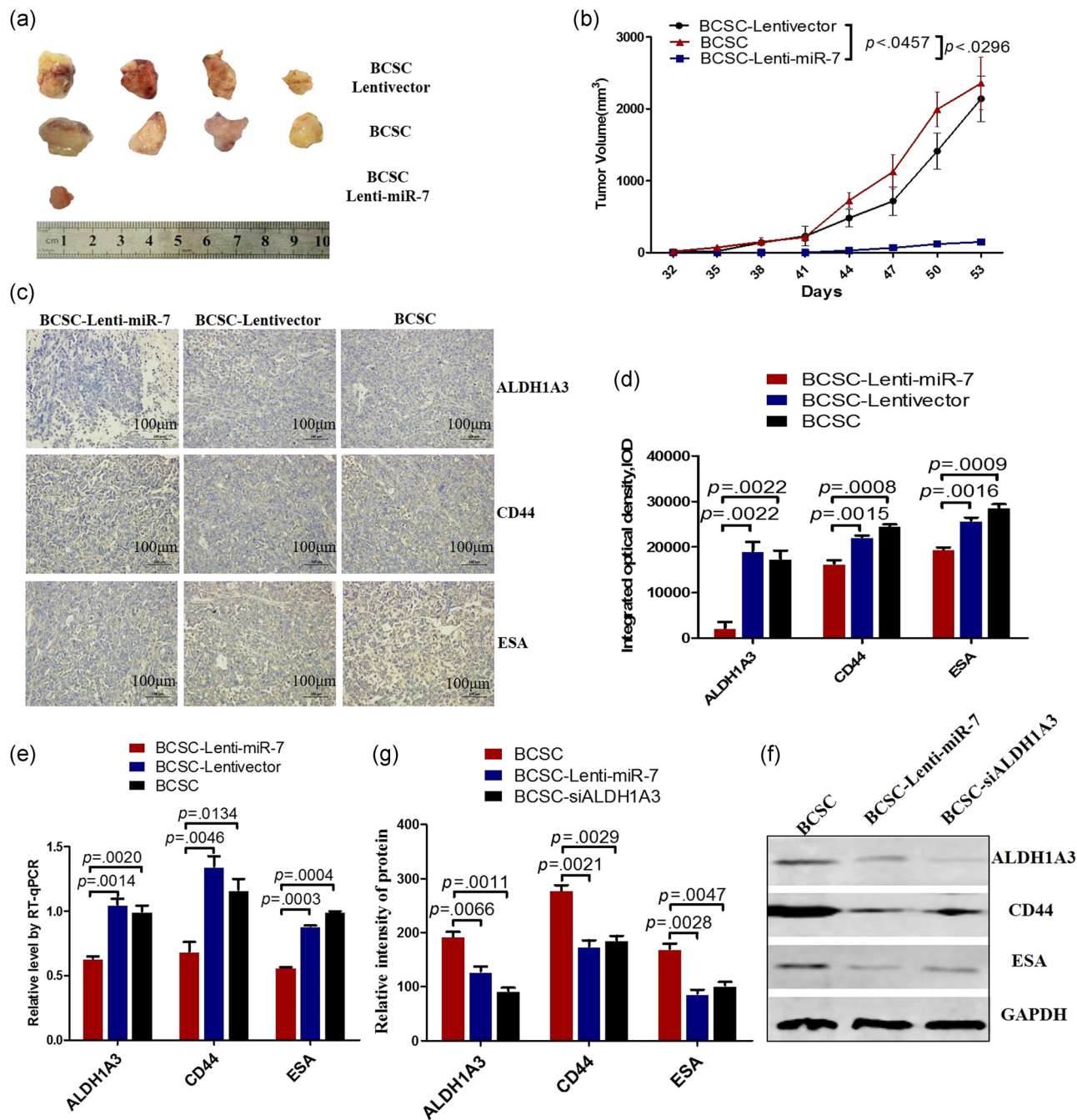

FIGURE 5 miR-7 inhibits breast cancer growth via suppressing the expressions of ALDH1A3, CD44, and ESA. (a) The tumor sizes dissected from the tumor bearing NOD/SCID mice 53 days after the injection of 2×10^5 CD44$^+$CD24$^-$ESA$^+$BCSCs. (b) Tumor dynamic growth drawing. (c) The expressions of ALDH1A3, CD44, and ESA in tumor tissues analyzed by IHC. (d) Semi-quantitatively analysis of the IHC results, referring to the differences as indicated. (e) RT-qPCR analysis of the expressions of ALDH1A3, CD44, and ESA in the tumor tissues. (f) western blot analysis of the expressions of ALDH1A3, CD44, and ESA in tumor tissues. (g) Semi-quantitatively analysis of western blot results. ALDH, aldehyde dehydrogenase; BCSC, breast cancer stem cell; ESA, epithelium specific antigen; NOD, nonobese diabetic; RT-qPCR, reverse transcription quantitative real-time polymerase chain reaction; SCID, severe combined immunodeficient

BCSC-Lentivector or BCSCs, which was statistically significant (Figure 5d).

Further, we evaluated these molecular expression by RT-qPCR and western blot assays. In accordance with the IHC results, the transcription expressions of ALDH1A3, CD44, and ESA were significantly reduced in the BCSCs infected with Lenti-miR-7 compared with the control cells (Figure 5e). The results were further supported by the results from the western blot (Figure 5f). The sample, from the tumor tissues in the mice injected by BCSC-Lenti-miR-7, indicated weaker bands of ALDH1A3, CD44, and ESA than those in the sample from the BCSC-Lentivector or BCSCs, which were statistically significant as is shown in Figure 5G.

4 | DISCUSSION

Since the CSCs are a subpopulation of cancer cells that are tightly associated with the chemoresistance and recurrence among cancer patients (Bak et al., 2018; Bledzka et al., 2017; Boo et al., 2016; Das & Law, 2018; Liu et al., 2018), we focused on the BCSCs in the present study and investigated the mechanisms of miR-7 reducing BCSC subpopulation.

Owing to the breast cancer cells with expression of ALDHs exhibiting stem cell-like features (Choi et al., 2018; Matsunaga et al., 2018; Okuda et al., 2013), we first adopted the ALDEFLUOR assay, a widely used method in detecting the activity of ALDH enzyme in various cancer types, to analyze the ALDH expression in breast cancer cell lines. As expected, the CD44$^+$CD24$^-$ and CD44$^+$CD24$^-$E-SA$^+$BCSCs revealed factually the higher ALDH activity than both BT549 and MDA-MB-231 cells, accompanied with a low miR-7 expression, especially in CD44$^+$CD24$^-$ ESA$^+$BCSCs. Given the different enzyme isoforms within the ALDH family having differential function, it was report that knockdown of ALDH1A3 in breast cancer cells decreased ALDH activity but did not alter proliferation, extravasation, or therapy resistance; while knockdown of ALDH1A1 reduced breast cancer cell metastatic behavior and therapy resistance (Croker et al., 2017; Marcato et al., 2011). Therefore, we selected ALDH isozyme, ALDH1A3 to evaluate the influence on breast cancer cell behaviors in the present study. Meanwhile, we enforced the miR-7 expression by using Lenti-miR-7 transduction to address the functional significance of the miR-7 in MDA-MB-231 cells. Our results indicated that the overexpression of miR-7 not only decreased ALDH1A3 expression but also reduced the expressions of the BCSC-related molecules CD44 and KLF-4 in MDA-MB-231 cells. Luciferase reporter assay results demonstrated that the putative miR-7 directly bond the 3′-UTR of ALDH1A3 vector resulting in inhibition of ALDH1A3 expression, which was further supported by western blot analysis (Figure 2). The results suggested that reduction of ALDH1A3 activity was associated with inhibition of BCSC stem-like molecule expression.

It was reported that ALDH1A3-induced differential etinoic acid signaling in breast cancer cells and the number of ALDH1A3-positive cells, a marker for breast cancer-initiating cells, which affected the rate of breast cancer progression (Bhat et al., 2019; Marcato et al., 2015). To this end, we downregulated ALDH1A3 expression by using RNA interference in MDA-MB-231 cells to evaluate the influence of ALDH1A3 on the expression of BCSC stem-like molecules. We found that the knockdown of ALDH1A3 reduced the CD44 and ESA expressions in MDA-MB-231 cells and decreased the BCSC subpopulation (Figure 3), suggesting the function of ALDH1A3 is closely related to CD44$^+$ESA$^+$BCSC subpopulation.

Based on these observations, we whereafter transduced the Lenti-miR-7 recombinant into CD44$^+$CD24$^-$ESA$^+$BCSCs to assess the influence of enforced miR-7 expression on BCSC-driven xenograft growth in NOD/SCID mice. The in vivo results indicated the mice injected with Lenti-miR-7-BCSCs initially developed tumor xenograft 10 days after injection. Surprisingly, the established tangible tumor xenografts in three mice were gradually shrunk and eventually vanished, only one tumor in mice kept very smaller tumor size than that in mice injected with Lenti-vector BCSCs or BCSCs. This suggested that miR-7 as anticancer reagent indeed inhibited breast cancer growth in mouse model.

In addition, consistent with the results of tumor tissue sections analyzed by immunohistochemistry, western blot analysis showed the molecular expressions of ALDH1A3, CD44, and ESA were significantly reduced in tumor tissues in the mice injected with Lenti-miR-7-BCSCs compared with the tumor tissues in the mice injected with Lenti-vector-BCSCs or BCSCs. On the basis of these findings, we conjectured that enforced miR-7 expression in BCSCs attenuated the BCSC's stem-like properties, reduced the ALDH1A3 activity, and decreased the BCSCs tumorigenicity, which revealed the miR-7 expression and ALDH1A3 levels has the close connection in breast cancer progression.

Our findings resembled a recent report by Matsunaga et al., where they proposed that ALDH activity is associated with the malignancy of cancer cells and is used for identification and isolation of BCSCs. Administration of ALDH inhibitor *N,N*-diethylaminobenzaldehyde increased the antitumor and antimetastatic effects in 4T1 cell-implanted mice (Choi et al., 2018; Matsunaga et al., 2018),which supported that the inhibition ALDH function suppressed implanted breast cancer in mouse model. In our current study, the decrease of ALDH1A3 expression led to reducing the BCSC subpopulation, which inhibited an implanted BCSC growth in mice. However, a few questions remain unanswered. For example, we do not know the inhibition of ALDH1A3 activity is how to affect the expressions of CD44 and ESA in MDA-MB-231 cells, which leads to the decrease of the BCSC subpopulation, and future study warrants to understand the mechanisms of the reducing BCSC subpopulation mediated by miR-7 overexpression.

In summary, our data represent the first attempt to demonstrate miR-7 attenuates the BCSCs characteristics and reduces the BCSC subset by decrease of ALDH1A3 activity, which inhibits BCSC-driven xenograft growth in mice. The findings suggest the ALDH1A3 is a potentially therapeutic target for treatment of breast cancer.

ACKNOWLEDGMENTS

CONFLICT OF INTERESTS

The authors declare that there are no conflict of interests.

AUTHOR CONTRIBUTIONS

M. P., M. L., C. Y., and J. D. designed and carried out the experiments, analyzed data and wrote the manuscript. F. Z., M. G., H. X., L. L., and L. W. performed real-time PCR and western blotting assays. M. L. and M. P. performed dual-luciferase reporter assay. M. G., H. X., L. L., and L. W. performed animal models and flow cytometry. J. D. analyzed data, wrote the manuscript, and provided overall supervision. All authors read and approved the final manuscript.

DATA AVAILABILITY

Data source can be provided upon reasonable request.

ORCID

Jun Dou http://orcid.org/0000-0001-6944-5874

REFERENCES

Asharani, P. V., Low, G., Kah Mun, M., Hande, P., & Valiyaveettil, S. (2009). Cytotoxicity and genotoxicity of silver nanoparticles in human cells. *ACS Nano*, *3*, 279–290.

Bak, M. J., Furmanski, P., Shan, N. L., Lee, H. J., Bao, C., Lin, Y., … Suh, N. (2018). Tocopherols inhibit estrogen-induced cancer stemness and OCT4 signaling in breast cancer. *Carcinogenesis*, *39*, 1045–1055. https://doi.org/10.1093/carcin/bgy071

Bhat, K., Sandler, K., Duhachek-Muggy, S., Alli, C., Cheng, F., Moatamed, N. A., … Pajonk, F. (2019). Serum erythropoietin levels breast cancer and breast cancer-initiating cells. *Breast Cancer Research*, *21*, 17.

Bledzka, K., Schiemann, B., Schiemann, W. P., Fox, P., Plow, E. F., & Sossey-Alaoui, K. (2017). The WAVE3-YB1 interaction regulates cancer stem cells activity in breast cancer. *Oncotarget*, *8*, 104072–104089.

de Boniface, J., Schmidt, M., Engel, J., Smidt, M. L., Offersen, B. V., & Reimer, T. (2018). What is the best management of cN0pN1(sn) breast cancer patients? *Breast Care*, *13*, 331–336.

Boo, L., Ho, W. Y., Ali, N. M., Yeap, S. K., Ky, H., Chan, K. G., … Cheong, S. K. (2016). MiRNA transcriptome profiling of spheroid-enriched cells with cancer stem cell properties in human breast MCF-7 cell line. *International Journal of Biological Sciences*, *12*, 427–445.

Cai, K., Jiang, L., Wang, J., Zhang, H., Wang, X., Cheng, D., & Dou, J. (2014). Downregulation of β-catenin decreases the tumorigenicity, but promotes epithelial-mesenchymal transition in breast cancer cells. *Journal of Cancer Research and Therapeutics*, *10*, 1063–1070.

Charafe-Jauffret, E., Ginestier, C., Iovino, F., Tarpin, C., Diebel, M., Esterni, B., … Wicha, M. S. (2010). Aldehyde dehydrogenase 1-positive cancer stem cells mediate metastasis and poor clinical outcome in inflammatory breast cancer. *Clinical Cancer Research*, *16*, 45–55.

Chen, D., Wang, J., Zhang, Y., Chen, J., Yang, C., Cao, W., … Dou, J. (2013). Effect of down-regulated transcriptional repressor ZEB1 on the epithelial-mesenchymal transition of ovarian cancer cells. *International Journal of Gynecological Cancer*, *23*, 1357–1366.

Chen, D., Zhang, Y., Wang, J., Chen, J., Yang, C., Cai, K., … Dou, J. (2013). MicroRNA-200c overexpression inhibits tumorigenicity and metastasis of CD117 + CD44 + ovarian cancer stem cells by regulating epithelial-mesenchymal transition. *Journal of Ovarian Research*, *6*, 50.

Chen, J. S., Wang, J., Chen, D. Y., Jiem, Y., Yang, C. P., Zhang, Y. X., & Dou, J. (2013). Evaluation of characteristics of CD44 + CD117 ovarian cancer stem cells in three dimensional basement membrane extract scaffold versus two dimensional monocultures. *BMC Cell Biology*, *14*, 7.

Chiyomaru, T., Yamamura, S., Fukuhara, S., Yoshino, H., Kinoshita, T., Majid, S., … Dahiya, R. (2013). Genistein inhibits prostate cancer cell growth by targeting miR-34a and oncogenic HOTAIR. *PLOS One*, *8*, e70372.

Choi, H. S., Kim, J. H., Kim, S. L., Deng, H. Y., Lee, D., Kim, C. S., … Lee, D. S. (2018). Catechol derived from aronia juice through lactic acid bacteria fermentation inhibits breast cancer stem cell formation via modulation Stat3/IL-6 signaling pathway. *Molecular Carcinogenesis*, *57*, 1467–1479.

Croker, A. K., Rodriguez-Torres, M., Xia, Y., Pardhan, S., Leong, H. S., … Allan, A. L. (2017). Differential functionalRolesofALDH1A1 and ALDH1A3 in mediating metastatic behaviorand therapy resistance of human breast cancer cells. *International Journal of Molecular Sciences*, *18*, 2039.

Cruz-Lozano, M., González-González, A., Marchal, J. A., Muñoz-Muela, E., Molina, M. P., Cara, F. E., … Granados-Principal, S. (2018). Hydroxytyrosol inhibits cancer stem cells and the metastatic capacity of triple-negative breast cancer cell lines by the simultaneous targeting of epithelial-to-mesenchymal transition, Wnt/β-catenin and TGFβ signaling pathways. *European Journal of Nutrition*, https://doi.org/10.1007/s00394-018-1864-1. Advance online publication.

Das, M., & Law, S. (2018). Role of tumor microenvironment in cancer stem cell chemoresistance and recurrence. *International Journal of Biochemistry and Cell Biology*, *103*, 115–124.

Dave, B., Granados-Principal, S., Zhu, R., Zhu, R., Benz, S., Rabizadeh, S., … Chang, J. C. (2014). Targeting RPL39 and MLF2 reduces tumor initiation and metastasis in breast cancer by inhibiting nitric oxide synthase signaling. *Proceedings of the National Academy of Sciences of the United States of America*, *111*, 8838–8843.

Dou, J., Pan, M., Wen, P., Li, Y., Tang, Q., Chu, L., … Gu, N. (2007). Isolation and identification of cancer stem-like cells from murine melanoma cell lines. *Cellular & Molecular Immunology*, *4*, 467–472.

Dou, J., Wang, Y., Yu, F., Yang, H., Wang, J., He, X., … Hu, K. (2012). Protection against Mycobacterium tuberculosis challenge in mice by DNA vaccine Ag85A-ESAT-6-IL-21 priming and BCG boosting. *International Journal of Immunogenetics*, *39*, 183–190.

Elliott, B., Millena, A. C., Matyunina, L., Zhang, M., Zou, J., Wang, G., … Khan, S. (2019). Essential role of JunD in cell proliferation is mediated via MYC signaling in prostate cancer cells. *Cancer Letters*, *448*, 155–167.

Ginestier, C., Hur, M. H., Charafe-Jauffret, E., Monville, F., Dutcher, J., Brown, M., ... Dontu, G. (2007). ALDH1 is a marker of normal and malignant human mammary stem cells and a predictor of poor clinical outcome. *Cell Stem Cell*, 1, 555–567.

Guo, L. W., Jiang, L. M., Gong, Y., Zhang, H. H., Li, X. G., He, M., ... Hu, X. (2018). Development and validation of nomograms for predicting overall and breast cancer-specific survival among patients with triple-negative breast cancer. *Cancer Management and Research*, 10, 5881–5894.

He, N., Kong, Y., Lei, X., Liu, Y., Wang, J., Xu, C., ... Liu, Q. (2018). MSCs inhibit tumor progression and enhance radiosensitivity ofbreast cancer cells by down- regulating Stat3 signaling pathway. *Cell Death & Disease*, 9, 1026.

Hosea, R., Hardiany, N. S., Ohneda, O., & Wanandi, S. I. (2018). Glucosamine decreases the stemness of human ALDH + breast cancer stem cells by inactivating STAT3. *Oncology Letters*, 16, 4737–4744.

Hu, W., Wang, J., Dou, J., He, X., Zhao, F., Jiang, C. ... Gu, N. (2011). Augmenting therapy of ovarian cancer efficacy by secreting IL-21 human umbilical cord blood stem cells in nude mice. *Cell Transplant*, 20, 669–680.

Huynh, F. C., & Jones, F. E. (2014). MicroRNA-7 inhibits multiple oncogenic pathways to suppress HER2Δ16 mediated breast tumor-igenesis and reverse trastuzumab resistance. *PLOS One*, 22, e114419.

Jeong, D., Ham, J., Park, S., Lee, S., Lee, H., Kang, H. S., & Kim, S. J. (2017). MicroRNA-7-5p mediates the signaling of hepatocyte growth factor to suppress oncogenes in the MCF-10A mammary epithelial cell. *Scientific Reports*, 13, 15425.

Liu, T., Xu, H., Huang, M., Ma, W., Saxena, D., Lustig, R. A., ... Fan, Y. (2018). Circulating Glioma Cells Exhibit Stem Cell-like Properties. *Cancer Research*, 78, 6632–6642.

Lugli, A., Iezzi, G., Hostettler, I., Muraro, M. G., Mele, V., Tornillo, L., ... Zlobec, I. (2010). Prognostic impact of the expression of putative cancer stem cell markers CD133, CD166, CD44s, EpCAM, and ALDH1 in colorectal cancer. *British Journal of Cancer*, 103, 382–390.

Luo, X. L., Xie, D. X., Wu, J. X., Wu, A. D., ... Gong, J. P. (2017). Detection of metastatic cancer cells in mesentery of colorectal cancer patients. *World Journal of Gastroenterology*, 23, 6315–6320.

Marcato, P., Dean, C. A., Liu, R. Z., Coyle, K. M., Bydoun, M., & Wallace, M. (2015). Aldehyde dehydrogenase 1A3 influences breast cancer progression via differential retinoic acid signaling. *Molecular Oncology*, 9, 17–31.

Marcato, P., Dean, C. A., Pan, D., Araslanova, R., Gillis, M., Joshi, M., ... Lee, P. W. (2011). Aldehyde dehydrogenase activity of breast cancer stem cells is primarily due to isoform ALDH1A3 and its expression is predictive of metastasis. *Stem Cells*, 29, 32–45.

Matsunaga, N., Ogino, T., Hara, Y., Tanaka, T., Koyanagi, S., & Ohdo, S. (2018). Optimized dosing schedule based on circadian dynamics of mouse breast cancer stem cells improves the antitumor effects of aldehyde dehydrogenase inhibitor. *Cancer Research*, 78, 3698–3708.

Mu, C., Wu, X., Zhou, X., Wolfram, J., Shen, J., Zhang, D., ...Shen, H. (2018). Chemotherapy sensitizes therapy-resistant cells to mild hyperthermia by suppressing heat shock protein 27 expression in triple negative breast cancer. *Clinical Cancer Research*, 24, 4900–4912.

Nagle, A. M., Levine, K. M., Tasdemir, N., Scott, J. A., Burlbaugh, K., Kehm, J. W., ... Lee, A. V. (2018). Loss of E-cadherin enhances IGF1-IGF1R pathway activation and sensitizes breast cancers to anti-IGF1R/InsR inhibitors. *Clinical Cancer Research*, 24, 5165–5177.

Okuda, H., Xing, F., Pandey, P. R., Sharma, S., Watabe, M., Pai, S. K., ... Watabe, K. (2013). miR-7 suppresses brain metastasis of breast cancer stem-like cells by modulating KLF4. *Cancer Research*, 73. 1434-1344.

Polonio-Alcalá, E., Rabionet, M., Guerra, A. J., Yeste, M., Ciurana, J., & Puig, T. (2018). Screening of additive manufactured scaffolds designs for triple negative breast cancer 3D cell culture and stem-like expansion. *International Journal of Molecular Sciences*, 19, 3148. pii: E3148.

Sterzyńska, K., Klejewski, A., Wojtowicz, K., Świerczewska, M., Nowacka, M., Kaźmierczak, D., ... Januchowski, R. (2018). Mutual expression of ALDH1A1, LOX, and collagens in ovarian cancer cell lines as combined CSCs-and ECM-related models of drug resistance development. *International Journal of Molecular Sciences*, 20, 54. pii: E54.

Wang, J., Cao, M. G., You, C. Z., Wang, C. L., Liu, S. L., Kai, C., & Dou, J. (2012). A preliminary investigation of the relationship between circulating tumor cells and cancer stem cells in patients with breast cancer. *Cellualar and Molecular Biology*, 58, OL1641–OL1645.

Wang, J., Chen, D., He, X., Zhang, Y., Shi, F., Wu, D., ... Dou, J. (2015). Downregulated lincRNA HOTAIR expression in ovarian cancer stem cells decreases its tumorgeniesis and metastasis by inhibiting epithelial-mesenchymal transition. *Cancer Cell International*, 15, 24.

Wang, X., He, X., Zhao, F., Wang, J., Zhang, H., Shi, F., ... Dou, J. (2014). Regulation gene expression of miR200c and ZEB1 positively enhances effect of tumor vaccine B16F10/GPI-IL-21 on inhibition of melanoma growth and metastasis. *Journal of Translational Medicine*, 12, 68.

Wang, Y., Tu, L., Du, C., Xie, X., Liu, Y., Wang, J., ... Luo, F. (2018). CXCR2 is a novel cancer stem-like cell marker for triple-negativebreast cancer. *OncoTargets and Therapy*, 11, 5559–5567.

Yang, C., Xiong, F., Wang, J., Dou, J., Chen, J., Chen, D., ... Gu, N. (2014). Anti-ABCG2 monoclonal antibody in combination with paclitaxel nanoparticles against cancer stem-like cell activity in multiple myeloma. *Nanomedicine*, 9, 45–60.

Zhang, H., Cai, K., Wang, J., Wang, X., Cheng, K., Shi, F., ... Dou, J. (2014). MiR-7, inhibited indirectly by lincRNA HOTAIR, directly inhibits SETDB1 and reverses the EMT of breast cancer stem cells by downregulating the STAT3 pathway. *Stem Cells*, 32, 2858–2868.

Zhou, J., Zhang, H., Gu, P., Margolick, J. B., Yin, D., & Zhang, Y. (2009). Cancer stem/progenitor cell active compound 8-quinolinol in combination with paclitaxel achieves an improved cure of breast cancer in the mouse model. *Breast Cancer Research and Treatment*, 115, 269–277.

Zhou, L., Sheng, D., Wang, D., Ma, W., Deng, Q., Deng, L., & Liu, S. (2018). Identification of cancer-type specific expression patterns for active aldehyde dehydrogenase (ALDH) isoforms in ALDEFLUOR assay. *Cell Biology and Toxicology*, 35, 161–177. https://doi.org/10.1007/s10565-018-9444-y